

Numerical Study on the Concrete Microstructure using Image-based Virtual Element Method

Hyeong-Tae Kim^a, Kyoungsoo Park^{a*}

^aDepartment of Civil and Environmental Engineering, Yonsei University, 50 Yonsei-ro, Seodaemun-gu, Seoul 120-749, Republic of Korea

*Corresponding author: k-park@yonsei.ac.kr

1. Introduction

Concrete is used in many parts of nuclear power plants (NPPs) because of its low cost, high shape flexibility, and radiation shielding ability. Concrete structures such as biological shield near the reactor are exposed to the high level of radiation during life-time. When the neutron fluence reaches a critical value, the compressive strength of concrete can rapidly decrease. Radiation-induced degradation has been demonstrated in previous researches [1, 2]. The influence of concrete microstructure on radiation-induced degradation is clear. Radiation-induced volume expansion (RIVE) of the aggregate causes radiation damage on the concrete [3]. In this study, a computational framework for the actual concrete microstructure analysis is proposed to consider the radiation-induced volume expansion of aggregates. The framework includes microstructural reconstruction using X-ray and Neutron CT, and image-based VEM technique [4, 5]. Then, uniaxial tension test and RIVE of aggregate are investigated to validate the accuracy and efficiency of the proposed methodology.

2. Image-based Virtual Element Method

In this section, a computational process for the concrete microstructure analysis is presented. The process includes microstructure reconstruction of actual concrete using X-ray and Neutron CT, and a mesh generation algorithm using polygonal elements based on the reconstructed image.

2.1 Concrete microstructure reconstruction using X-ray and Neutron CT image

The concrete microstructure is reconstructed using the complementarity of X-ray and Neutron CT. X-rays are sensitive to the density of matter, and Neutrons to hydrates. Therefore, X-ray and Neutron CT images of same concrete cross-section may differ as shown in Fig. 1. These differences demonstrate as red and green areas in Fig. 1(c). Aggregates in this area may not be distinct using only a single type of CT. In this study, X-ray and neutron CT images for the concrete specimens are obtained. Next, three material phases (void, paste, and aggregate) are identified using image segmentation techniques. Finally, concrete microstructure is reconstructed through noise canceling and image registration [4].

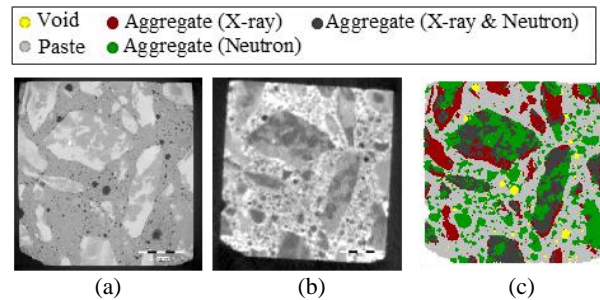


Fig. 1. (c) Reconstructed concrete microstructure using the complementarity of (b) X-ray CT and (c) Neutron CT image.

2.2 Polygonal mesh generation algorithm

The mesh generation algorithm is proposed to generate a discretized concrete microstructure mesh with polygonal elements based on the image. Mesh generation according to the geometrical representation of concrete microstructure is significantly difficult because of the complexity of the shape and wide range of length scales in the particles. Virtual element technique can be handling the arbitrary shape of elements such as non-convex shape in one domain, so the discretization has much more flexibility. The mesh generation examples are demonstrated in Fig. 4. First, microstructure mesh composed of aggregate and paste is generated based on the image. Next, to achieve the desired level of accuracy, a homogeneous mesh with a certain size of elements is generated. Finally, polygonal meshes are generated by integrating these two meshes [5].

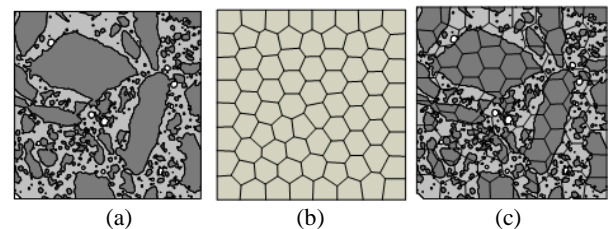


Fig. 2. Schematics of the polygonal mesh generation with a: (a) microstructure mesh, (b) homogeneous mesh, and (c) integration of homogeneous and microstructure mesh.

3. Numerical Examples

The efficiency and accuracy of the presented framework is validated by the numerical result for the uniaxial tension and RIVE of aggregate example.

3.1 Uniaxial tension test

Concrete microstructure is the rectangular domain, as shown in Fig. 3. Image size is $1,304 \text{ pixel} \times 1,304 \text{ pixel}$. The uniform displacement of $1.798 \text{ }\mu\text{m}$ is applied along the normal to the upper edge under the plain stress condition. Gabbro aggregate is classified into four types of rock-forming minerals, which are plagioclase (green), pyroxene (black), quartz (blue), and hornblende (red), respectively. The elastic moduli of the aggregate and paste are selected as 92.0 GPa, 97.9 GPa, 84.1 GPa, 101.5 GPa, and 20 GPa, respectively; the Poisson's ratio of the aggregate and paste are 0.282, 0.338, 0.099, 0.264, and 0.2, respectively.

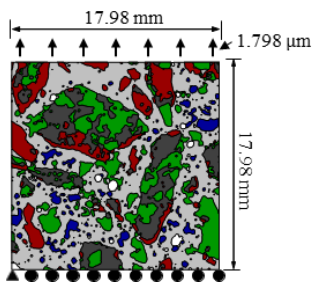


Fig. 3. Geometry and boundary conditions of the concrete microstructure under uniaxial tension test.

To demonstrate the convergence of computational results under mesh refinement, the computational results with the image-based VEM are compared with the reference solution. Fig. 4 show the relative error of computed macroscopic elastic modulus and total strain energy. Total strain energy error is calculated by H-type skeleton norm. These results are converges to the reference solution under the mesh refinement.

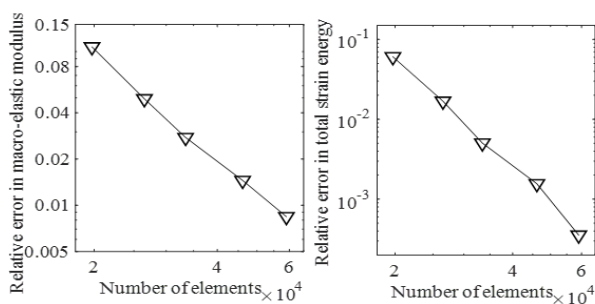


Fig. 4. Relative error of the (a) macro-elastic modulus, and (b) total strain energy according to the number of elements.

3.2 RIVE of aggregate

The concrete microstructure domain used in the RIVE of aggregate example is the same as the uniaxial tensile test previously. Then, the volumetric strain of aggregate is applied according to the fluence of neutrons under the plane strain condition. Initial volumetric strain according to the RIVE is determined

based on the previous research [6]. The number of elements in the polygon mesh is the most refinement mesh in the previous example. The numerical results demonstrate that as the fluence of neutron radiation increases, the entire volume of concrete increases, which is matched with the experimental results (Fig 5).

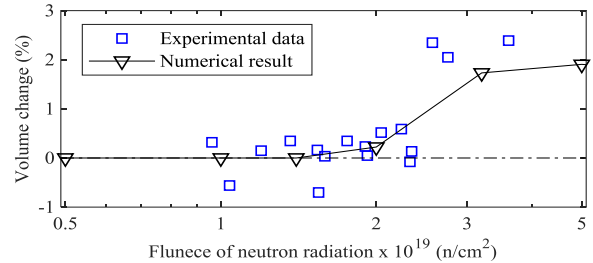


Fig. 5. Volume change according to the fluence of neutron radiation on the experimental data and numerical result

4. Conclusion

Image-based VEM using X-ray and Neutron CT is proposed for actual concrete microstructure analysis efficiently. It improves the accuracy of concrete microstructure by using the complementarity of X-ray and Neutron CT. Based on the mesh generation algorithm, a polygonal mesh is successfully generated according to the level of accuracy required by computational analysis. Concrete microstructure analysis under uniaxial tension and RIVE of aggregate is numerically investigated using the proposed computational framework. The proposed image-based VEM provides a result efficiently, and well-math with the distribution of experimental data.

ACKNOWLEDGEMENTS

This work was supported by the National Research Foundation of Korea (NRF) grant funded by the Korea government (Ministry of Science and ICT) (No. RS-2022-0014450).

REFERENCES

- [1] K. G. Field, I. Remec, and Y. Le Pape, Radiation effects in concrete for nuclear power plants – Part I: Quantification of radiation exposure and radiation effects, Nuclear Engineering and Design, Vol.282, p. 126-143, 2015.
- [2] K. Willam, Y. Xi, and D. Naus, A review of the effects of radiation on microstructure and properties of concrete used in nuclear power plants, U.S. Nuclear Regulatory Commission, NUREG/CR-7171, 2013.
- [3] T. M. Rosseel, I. Maruyama, Y. Le Pape, O. Kontani, A. B. Giorla, I. Remec, J. J. Wall, M. Sircar, C. Andrade, and M. Ordóñez, Review of the current state of knowledge on the effects of radiation on concrete, Journal of Advanced Concrete Technology, Vol.14(7), p.368-383, 2016.
- [4] H. T. Kim, D. F. Tiana Razakamandimby R, V. Szilágyi, Z. Kis, L. Szentmiklósi, M. A. Glinicki, and K. Park,

Reconstruction of concrete microstructure using complementarity of X-ray and neutron tomography. *Cement and Concrete Research*, Vol.148, p.106540, 2021.

[5] H. T. Kim, and K. Park, Microstructure analysis of concrete with poly-mineral aggregate using image-based VEM, (in preparation).

[6] Y. Le Pape, M. H. Alsaïd, and A. B. Giorla, Rock-forming minerals radiation-induced volumetric expansion-revisiting literature data, *Journal of Advanced Concrete Technology*, Vol.16(5), p.191-209, 2018.